

Synthesis, Anticancer Activity, and Molecular Docking Studies of Novel Substituted Isoxazole Derivatives Tethered 4-Nitroimidazole

Sadeekah O. Saber,^{*,[a, g]} Najim A. Al-Masoudi,^{†,[b]} Yaseen A. Al-Soud,^{*,[c]} Luay Abu Qatouseh,^[d] Bahjat A. Saeed,^[e] and Raed A. Al-Qawasmeh^{*,[f, g]}

A series of 4-nitroimidazole-piperazine conjugated 3,5-disubstituted isoxazole analogs **9a–o** were synthesized using nitrile oxide/alkyne cycloadditions (NOAC) with good yields. The antiproliferative activities of these compounds were evaluated against breast cancer cell lines MCF-7 and MDA-MB-231, as well as prostate cancer cell lines PC-3 and DU-145. Notably, compounds **9a**, **9j**, **9k**, and **9o** exhibited significant antiproliferative effects against MCF-7 cells, with IC₅₀ values ranging from 0.052 to 0.012 μ M, while no activity was observed against the MDA-

MB-231 cell line. Additionally, compounds **9a**, **9d**, **9g**, **9j**, and **9k** showed significant cytotoxicity against PC-3 cells, with IC₅₀ values between 0.156 and 0.041 μ M. Compounds **9a**, **9j**, **9k**, and **9o** also demonstrated antiproliferative activity against DU-145 cells, with IC₅₀ values ranging from 1.18 to 0.356 μ M. Molecular docking studies revealed that compound **9a** exhibited strong binding interactions with human protein receptors ER, PR, and HER2, while compound **9j** showed significant binding affinity with the androgen receptor CYP450 17A1.

1. Introduction

Imidazole, a five-membered aromatic ring, is an organic alkaloid that serves as a crucial pharmacophore in drug discovery due to its derivatives' wide range of biological and pharmacological activities.^[1,2] Biological studies have uncovered a variety of substituted imidazoles that display a broad spectrum of biological activities, including antimicrobial,^[3,4] anti-HIV,^[5] antihypertensive,^[6] antifungal,^[7] anticonvulsant,^[8]

anticoagulant,^[9] and anti-tuberculosis^[10] properties. Several drugs with an imidazole backbone are used as therapeutic agents for the treatment of various diseases. Examples include dacarbazine (DTIC) (an alkylating agent) (Figure 1a),^[11] temozolomide (Temodar) (an alkylating agent) (Figure 1b),^[12] clotrimazole (an antifungal agent),^[13] Flagyl (an antibiotic),^[14,15] misonidazole (a radiosensitizer and antineoplastic),^[16] cimetidine (a histamine H₂ receptor antagonist),^[17] as well as secnidazole and tinidazole (used for bacterial vaginosis).^[18,19] Additionally, nitroimidazole analogs form an important class of heterocyclic compounds with diverse biological activities.^[20–23]

Isoxazole derivatives have demonstrated a broad range of biological activities and therapeutic potential,^[24–26] including anticancer^[27] and anticonvulsant^[28] properties, among others. Their anticancer effects are mediated through various pathways, such as regulating the cell cycle, inducing apoptosis, inhibiting aromatase, tubulin, or phospholipase A₂. In addition, some isoxazole derivatives have been recognized as immune function regulators.^[29] Eid et al.^[30] reported the synthesis and biological evaluation of novel isoxazole-amide analogs as anticancer and antioxidant agents; meanwhile, Wazalwar et al.^[31] synthesized isoxazole derivatives from 3-chloroacrylaldehyde and cinnamaldehyde, identifying several as CYP1A2 inhibitors. The isoxazole backbone and its derivatives are widely regarded as a privileged scaffold in several well-known drugs. Notable examples include Tivozanib (Figure 1c),^[32] a treatment for advanced renal cell carcinoma (kidney cancer); Leflunomide (Figure 1d),^[33] an immunosuppressive disease-modifying antirheumatic drug (DMARD) that inhibits de novo pyrimidine nucleotide biosynthesis; and cloxacillin (Figure 1e),^[34] an antibiotic used to treat bacterial infections. Wang et al.^[35] provided an extensive review of the pharmacological importance of the isoxazole/isoxazoline scaffold in the structural modification of natural products.

[a] S. O. Saber

Faculty of Pharmacy, Jerash University, Amman-Irbid international highway, Jerash 26150, Jordan
E-mail: s.saber@jpu.edu.jo

[b] N. A. Al-Masoudi[†]

Department of Chemistry, College of Science, University of Basrah, Basrah, Iraq

[c] Y. A. Al-Soud

Chemistry Department, Faculty of Science, University of Al al-Bayt, Al-Mafraq, Jordan
E-mail: alsoud@aabu.edu.jo

[d] L. Abu Qatouseh

Faculty of Pharmacy, University of Petra, Amman, Jordan

[e] B. A. Saeed

Department of Chemistry, College of Education for Pure Science, University of Basrah, Basrah, Iraq

[f] R. A. Al-Qawasmeh

Pure and Applied Chemistry Group, Department of Chemistry, College of Sciences, University of Sharjah, Sharjah 27272, UAE
E-mail: ralqawasmeh@sharjah.ac.ae

[g] S. O. Saber, R. A. Al-Qawasmeh

Department of chemistry, School of Science, The University of Jordan, Amman 11942, Jordan

[[†]] present address: 78464 Konstanz, Germany

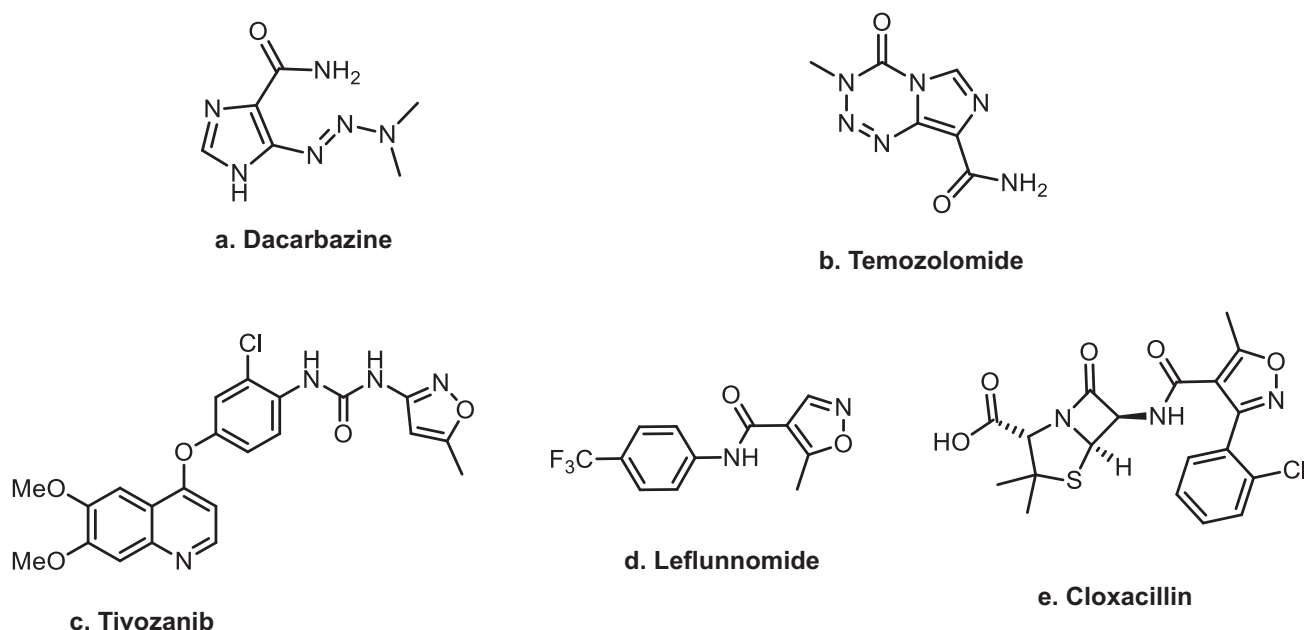


Figure 1. Some drugs based on imidazole and isoxazole derivatives.

In view of the varied pharmacological activities of nitroimidazole and isoxazole derivatives and following up on our previous research on imidazole analogues with anticancer activity,^[36,37] we now report here novel nitroimidazole–piperazine conjugated isoxazole derivatives, with evaluation of their anticancer activity and present findings from a molecular docking study.

2. Results and Discussion

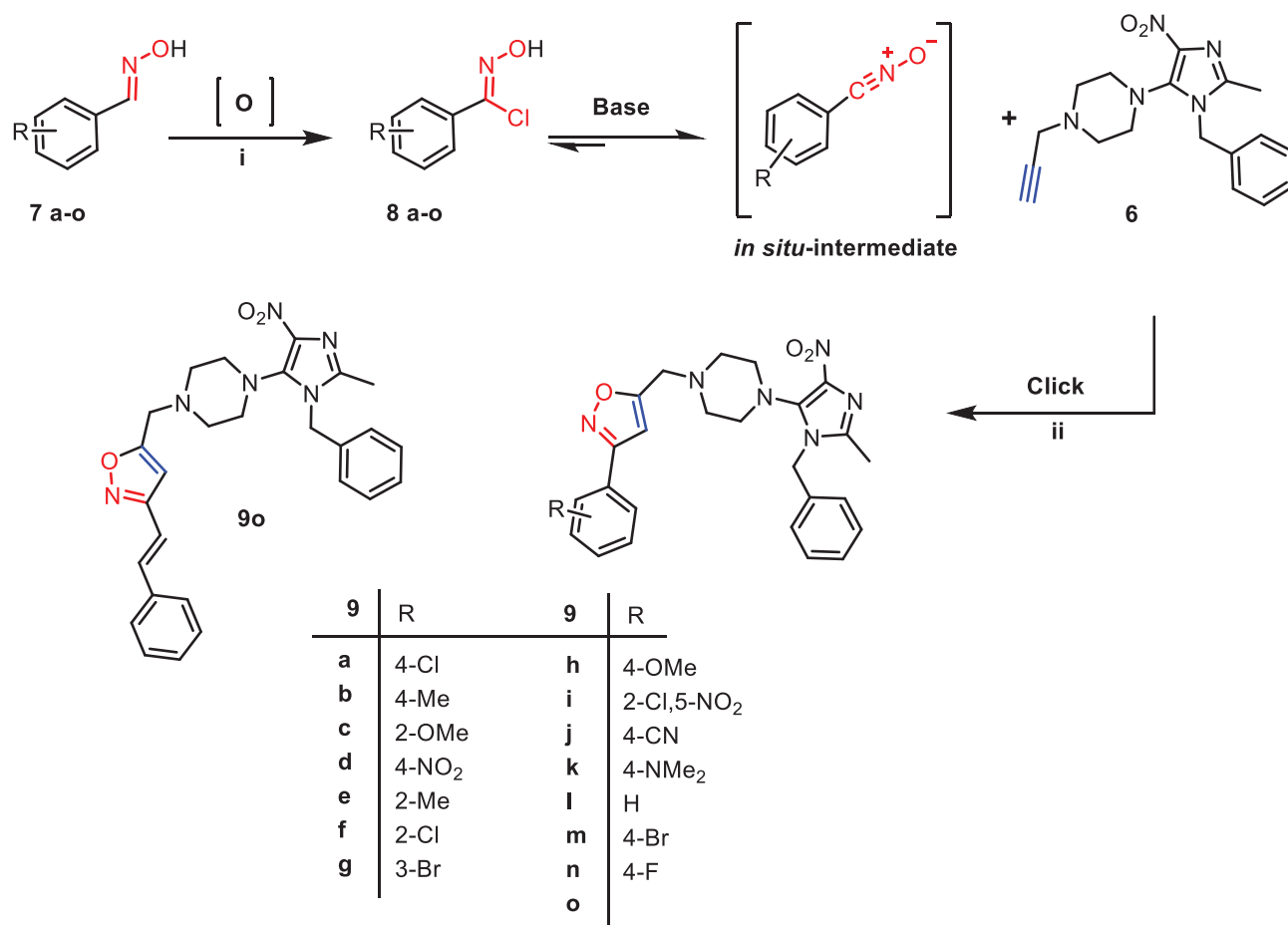
2.1. Chemistry

The 3,5-disubstituted isoxazoles have been explored for the last 50 years as a potential biologically active scaffold. A previous report from our group demonstrated that nitroimidazole tethered with an aliphatic linker led to the development of reliable hybrid biologically active compounds.^[38,39] Thus, we selected 1-(*N'*-benzyl-2-methyl-4-nitro-1*H*-imidazol-5-yl)-4-(prop-2-yn-1-yl)piperazine (**6**), previously described,^[37] as the starting material for synthesizing new 4-nitro-piperazine-conjugated substituted isoxazole derivatives. The synthesis involved four sequential steps, beginning with commercially available 2-methyl-4(5)-nitro-1*H*-imidazole. This process included selective benzylation at the nitrogen atom, followed by bromination and subsequent displacement of bromine with piperazine, yielding piperazinyl-nitroimidazole, which was then propargylated to obtain compound **6**. Treatment of **6** with nitrosyl compounds generated in situ from *N*-hydroxybenzimidoyl chlorides **8a–o** using *N*-chlorosuccinimide (NCS) in pyridine, in the presence of CuI, facilitated a click 1,3-dipolar cycloaddition, yielding the desired products **9a–o** in 96%–48% yield (Scheme 1).

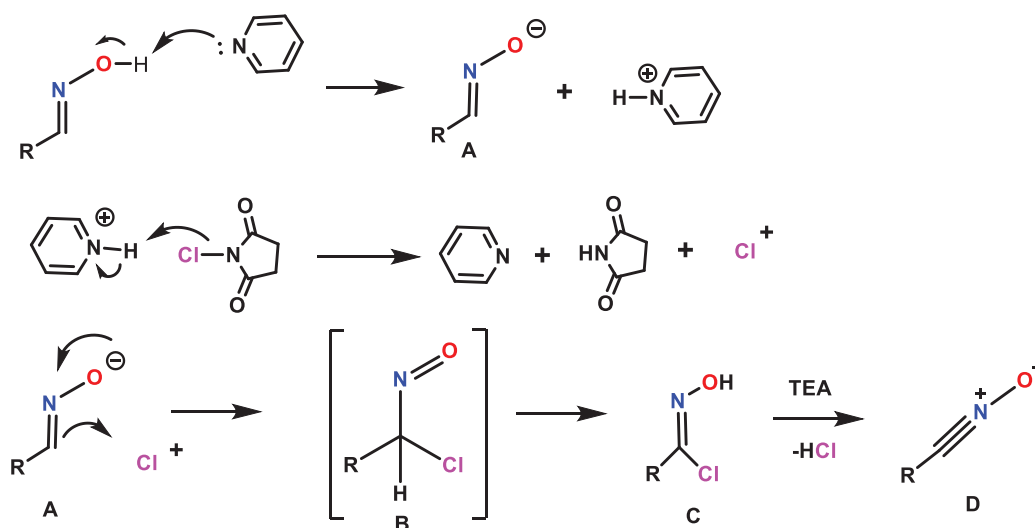
The 1,3-dipolar cycloaddition of nitrile oxides to unsaturated C=C bonds has proven to be highly effective for synthesizing isoxazoles.^[40] In this process, the copper-catalyzed

synthesis selectively yielded 3,5-disubstituted regioisomers **9a–o**. The isoxazole “left-wing” moiety was created through nitrile oxide/alkyne cycloaddition (NOAC), utilizing nitrile oxides generated in situ by dehalogenating *N*-hydroxybenzimidoyl chlorides **8a–o** in the presence of triethylamine as a base. Following Liu’s 1980 methodology,^[41] compounds **8a–o** were converted into nitrile oxides (Scheme 2), which then underwent catalytic cycloaddition with terminal alkyne **6**, resulting in the formation of the isoxazole derivatives **9a–o** (Scheme 1). The plausible mechanism for the formation of aryl-nitrone from oxime derivatives in the presence of NCS and pyridine involves a multi-step process. Initially, the reaction generates intermediate A along with a pyridinium salt. In the presence of NCS, this salt loses a proton, forming a chloride cation. Intermediate A then undergoes rearrangement facilitated by the chloride cation to produce intermediate B, which subsequently leads to intermediate C. Upon treatment with triethylamine (TEA) as a base, intermediate C is converted into the final nitrone intermediate D, as shown in Scheme 2. In summary, pyridine acts as a base to facilitate the reaction, while NCS functions both as an oxidizing agent and as a source of chloride.

The structures of the newly synthesized compounds **9a–o** were confirmed by their ¹H- and ¹³C NMR spectra, which displayed consistent patterns. In the ¹H NMR spectra of **9a–o**, the disappearance of the alkyne proton signal (–C≡CH) from compound **6**, previously observed around $\delta = 2.5$ ppm was noted. This was accompanied by the appearance of new signals in the aromatic region at the region $\delta = 6.0$ –7.0 ppm, characteristic of the isoxazole moiety. A downfield shift to $\delta = 0.5$ –0.7 ppm was attributed to the methylene protons (N–CH₂–C) of the isoxazole ring. The new signals in the aromatic region exhibited multiplicities and coupling constants that reflect the substitution patterns in the newly formed aromatic moiety. For example, compound **9m** exhibited a typical *para*-substituted pattern in its



Scheme 1. Reagents and conditions: (a) NCS, pyridine, DMF-CH₂Cl₂ (1:6 v/v), r.t, 12 h; (b) 1.0 mol% CuI / TEA, toluene, r.t, >12 h.



Scheme 2. The plausible reaction pathway through the reaction of benzaldoxime and NCS.

¹H-NMR spectrum. The aromatic protons H_{arom.}-3''' and H_{arom.}-5''' appeared as doublets at $\delta = 7.57$ ppm, while H_{arom.}-2''' and H_{arom.}-6''' also appeared as doublets at $\delta = 7.66$ ppm. The proton at H_{isoxazole}-4''' of the isoxazole resonated as a singlet at $\delta = 6.48$ ppm; meanwhile, the 12 *N*-methylene protons were

represented by eight protons appearing as two broad, weak singlets at $\delta = 2.55$ and 3.07 ppm, corresponding to the piperazine protons. The remaining four methylene protons resonated as a singlet at $\delta = 5.05$ ppm, associated with the benzyl group attached to the nitroimidazole ring, while the methylene pro-

tons attached to the piperazine and isoxazole rings resonated at $\delta = 3.73$ ppm. The ^{13}C NMR spectra were consistent with the proposed structures of compounds **9a–o**. The triple bond signals from compound **6**, previously observed at $\delta = 76.3$ and 79.6 ppm, were replaced by three characteristic signals corresponding to the isoxazole ring. The resonances in the regions $\delta \sim 170$, 101 , and 161 ppm were attributed to carbon atoms of the isoxazole ring C-3''', C-4''', and C-5''', respectively. For example, compound **9m** showed two new signals at $\delta = 170.3$ and 161.5 ppm assigned to the quaternary carbons $\text{C}_{\text{isoxazole-3'''}}$ and $\text{C}_{\text{isoxazole-5'''}}$, respectively, while a third signal at $\delta = 101.2$ ppm was attributed to $\text{C}_{\text{isoxazole-4'''}}$. These signals are key markers of isoxazole ring formation. The assignment of these signals was based on DEPT-NMR. In addition, a pronounced downfield shift is observed for the methylene carbon located between the isoxazole and piperazine rings, shifting from $\delta = 46.4$ ppm in compound **6** to $\delta = 53.4$ ppm in compound **9m**, highlighting a significant aspect of this synthesis. All other carbon signals appeared at their expected chemical shifts with only minor variations compared to compound **6**. Moreover, the methylene carbons in the piperazine ring maintained their characteristic pattern, where the $\text{C}_{\text{piperazine-3''}}$ and $\text{C}_{\text{piperazine-5''}}$ signals overlapped with the isoxazole methylene carbon. A noticeable reduction in the $\text{C}_{\text{piperazine-2''}}$ and $\text{C}_{\text{piperazine-6''}}$ signals was observed in the DEPT-135 experiment. On the other hand, all protons were unambiguously assigned based on HMQC and HMBC analysis. The weak, broad signals of $\text{H}_{\text{piperazine-2''}}$ and $\text{H}_{\text{piperazine-6''}}$ in the HMQC spectrum for the piperazine ring can be attributed to restricted rotation around the $\text{N}^1\text{-C-5}$ bond of the nitroimidazole moiety. This restriction hinders the dynamic equilibrium between the two chair conformations of the piperazine ring, resulting in clear correlations between these protons and the shrinking $\text{C}_{\text{piperazine-2''}}$ and $\text{C}_{\text{piperazine-6''}}$ carbon signals.

The gradient-selected HMBC spectrum^[42] of compound **9m** showed a $^2J_{\text{C,H}}$ coupling between $\text{CH}_2\text{-Ph}$ protons at $\delta = 5.05$ ppm and C-2 of the nitroimidazole group at $\delta = 140.0$ ppm, in addition to a $^3J_{\text{C,H}}$ coupling between the methylene protons of $\text{CH}_2\text{-C}_{\text{isoxazole-5'''}}$ at $\delta = 3.73$ ppm and carbons atoms of piperazine moiety ($\text{C}_{\text{piperazine-5''}} + \text{C}_{\text{piperazine-6''}}$) at $\delta = 49.1$ ppm. A $^2J_{\text{C,H}}$ coupling between $\text{CH}_2\text{-C}_{\text{isoxazole-5'''}}$ at $\delta = 3.73$ ppm and C-4''' of the isoxazole ring at $\delta = 101.2$ ppm was witnessed; meanwhile, a $^3J_{\text{C,H}}$ coupling between $\text{CH}_2\text{-C}_{\text{isoxazole-5'''}}$ at $\delta = 3.73$ ppm and $\text{C}_{\text{isoxazole-5'''}}$ of the same ring at $\delta = 161.5$ was observed (Figure 2).

HRMS analysis of **9m** gave the molecular ion of $[\text{M} + \text{Na}]^+ = 559.10594$ corresponding to the molecular formula of $\text{C}_{25}\text{H}_{25}\text{BrN}_6\text{O}_3\text{Na}$. The molecular mass clearly confirms the success of the construction of our new compound.

2.2. Biological Evaluation

All the newly synthesized compounds were tested against a panel of cancer cell lines, namely, human breast adenocarcinoma (MCF-7) (HTB-22TM), epithelial breast cancer (MDA-MB-231), human androgen-resistant (PC-3), and androgen-sensitive (DU-145) prostate cancer, (Table 1), using MTT assay^[43] and the antitumor drugs paclitaxel and docetaxel as reference drugs. The

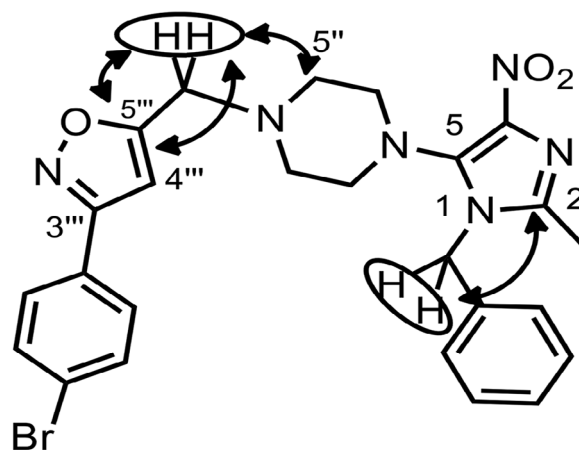
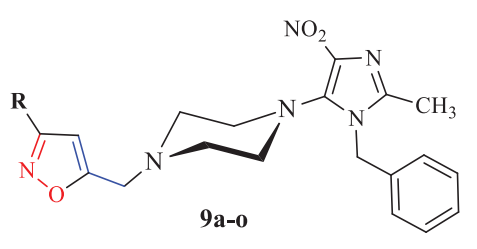


Figure 2. Selected HMBC correlations at compound **9m**.

compounds exhibited strong activity against both MCF-7 and PC-3 cell lines, with IC_{50} values ranging from nanomolar to sub-micromolar concentrations. Table 1 showed that compounds **9d**, **9g**, and **9m** exhibited potent activity with ($\text{IC}_{50} < 0.20$ μM), While compounds **9a** and **9j** exhibited a promising activity against the (MCF-7) cell line with ($\text{IC}_{50} = 0.012$ and 0.052 μM) respectively. Furthermore, the selectivity toward (MCF-7) cancer cell lines has encouraged us to investigate these two compounds and reveal their biological target at the molecular level. Compounds **9a**, **9j**, **9k**, and **9o** displayed significant cytotoxic activity against MCF-7 cell lines, with IC_{50} values varied between 0.052 and 0.01 μM , meanwhile the IC_{50} values of the other analogs against MCF-7 ranged between 0.585 and 0.112 μM . Regarding the substituted isoxazole substituents, Table 1 clearly showed that substituting with 4-Cl, 4-CN, 4-Me. or $\text{PhC}\equiv\text{C}$ groups significantly enhanced the inhibitory effect on MCF-7 cell lines. In contrast, most synthesized compounds were inactive against MDA-MB-231 breast cancer cells, except for **9a**, **9j**, and **9k**, which exhibited IC_{50} values of 10.966 , 10.985 , and 11.65 μM , respectively. Additionally, compounds **9a**, **9d**, **9g**, **9j**, **9k**, and **9o** demonstrated strong cytotoxic activity against the prostate cancer cell line PC-3, with IC_{50} values ranging from 0.064 to 0.043 μM . Moreover, compounds **9j**, **9k**, and **9o**, featuring 4-cyano, 4-Me, and $\text{PhCH}=\text{CH}_2$ groups on the isoxazole–piperazine ring, respectively, also exhibited good cytotoxic effects against the DU-145 prostate cancer cell line, with IC_{50} values of 0.752 , 0.356 , and 0.476 μM , respectively. In contrast, the remaining compounds in the series showed activity against DU-145, with IC_{50} values ranging from 1.18 to 17.041 μM .

3. In Silico Studies

There is a significant unfulfilled need for targeted therapies in patients with triple-negative breast cancer (TNBC). This study aimed to investigate potential biomarkers for sensitivity to 5-nitroimidazole-piperazine conjugated isoxazole derivatives, focusing on estrogen and progesterone receptors (ER and PR), as well as HER2 signaling in human breast cancer cell lines. AutoDock4^[44] was utilized for docking calculations, with results

Table 1. Half-maximal inhibitory concentrations (IC_{50}) of tested compounds in human breast adenocarcinoma, epithelial breast cancer, human androgen-resistant, and androgen-sensitive values expressed in (μ M).


9a-o

IC_{50} (μ M)		Breast Cancer Cells		Prostate Cancer Cells	
R	Compound ID	MCF-7	MDA-231	PC-3	DU-145
<i>p</i> -ClC ₆ H ₄ -	9a	0.012	10.966	0.043	1.18
<i>p</i> -CH ₃ C ₆ H ₄ -	9b	0.372	94.571	0.112	8.08
<i>o</i> -OMeC ₆ H ₄ -	9c	0.372	94.552	0.149	9.6
<i>p</i> -NO ₂ C ₆ H ₄ -	9d	0.112	80.163	0.093	3.16
<i>o</i> -CH ₃ C ₆ H ₄ -	9e	0.585	185.84	0.262	17.041
<i>o</i> -ClC ₆ H ₄ -	9f	0.372	132.839	0.156	8.281
<i>m</i> -BrC ₆ H ₄ -	9g	0.112	80.163	0.064	2.097
<i>p</i> -OMeC ₆ H ₄ -	9h	0.585	94.751	0.112	15.379
2-Cl,5-NO ₂ C ₆ H ₃ -	9i	0.162	115.34	0.156	2.944
<i>p</i> -CNC ₆ H ₄ -	9j	0.052	10.985	0.041	0.752
<i>p</i> -(Me) ₂ NC ₆ H ₄ -	9k	0.052	11.65	0.064	0.356
C ₆ H ₅ -	9l	0.156	80.163	0.156	2.365
<i>p</i> -BrC ₆ H ₄ -	9m	0.112	115.34	0.112	2.841
<i>p</i> -FC ₆ H ₄ -	9n	0.156	94.751	0.149	3.455
PhHC = CH-	9o	0.052	20.052	0.064	0.476
	Paclitaxel	0.021	0.031	0.01	0.07
	Docetaxel	0.23	0.105	0.01	0.1

^{a)} The IC_{50} s were determined by MTT method. Assays were performed duplicate in parallel.

visualized and analyzed using MGLTools. The receptor molecules were prepared by removing water molecules and performing correction and 3D protonation refinement.

In our quest for a new breast anticancer lead derivative, we have selected compound **9a** for molecular docking studies with ER (PDB: 3ERT), PR (PDB: 3G8O), and HER2 (PDB: 3PP0) due to its low IC_{50} among the 5-nitroimidazole series. The three-dimensional structures of these hormone receptors were used for docking with AutoDock 4. Ligands were ranked based on the highest energy of their best conformations, with compound **9a** yielding binding energy scores of -10.3 , -13.32 , and -9.02 kcal/mol for ER, PR, and HER2, respectively (Table 2), indicating selective binding to the active sites of these hormone receptors.

Figure 3a–c illustrates the docking results, showing the precise positioning of compound **9a** in relation to ER, PR, and HER2 (PDB: 3ERT, 3G8O, and 3PP0, respectively). Docking of **9a** with ER revealed a hydrogen bond between a nitrogen atom of the isoxazole group and Thr347 (2.932 Å). Docking of **9a** with PR showed a hydrogen bond between Mit801 and one oxygen atom of the nitro residue (1.999 Å), along with a π – π interaction between the

Ph-Cl group and Ph864. For HER2, docking results demonstrated a hydrogen bond between Arg766 and one oxygen atom of the nitro group.

The human androgen receptor (AR) is a key therapeutic target for prostate cancer (PCa). The 3D structures of human AR were sourced from the Protein Data Bank (PDB: 3RUK and 1E3G). Compound **9j** was identified as a potential new inhibitor of the human AR. The binding energy scores for **9j** were -10.12 and -8.17 kcal/mol, indicating good selectivity and potency for binding to the active site of the protein receptor pockets (3RUK and 1E3G).

As illustrated in Figure 3d (PDB: 3RUK), the positioning of the 5-nitroimidazole backbone within the binding pocket allows the nitro group of the imidazole scaffold to form a hydrogen bond with Ala105 (2.045 Å). Additionally, π – π stacking interactions between HEM600 and both the PhCN and isoxazole moieties were observed. Furthermore, (Figure 3e) showed the docking analysis for compound **9j** with the human androgen receptor (PDB: 1E3G), revealing a hydrogen bond (1.708 Å) between the oxygen atom of the nitro residue and Lys808, along with π – π interactions between Trp751 and both the phenyl (PhCN) and

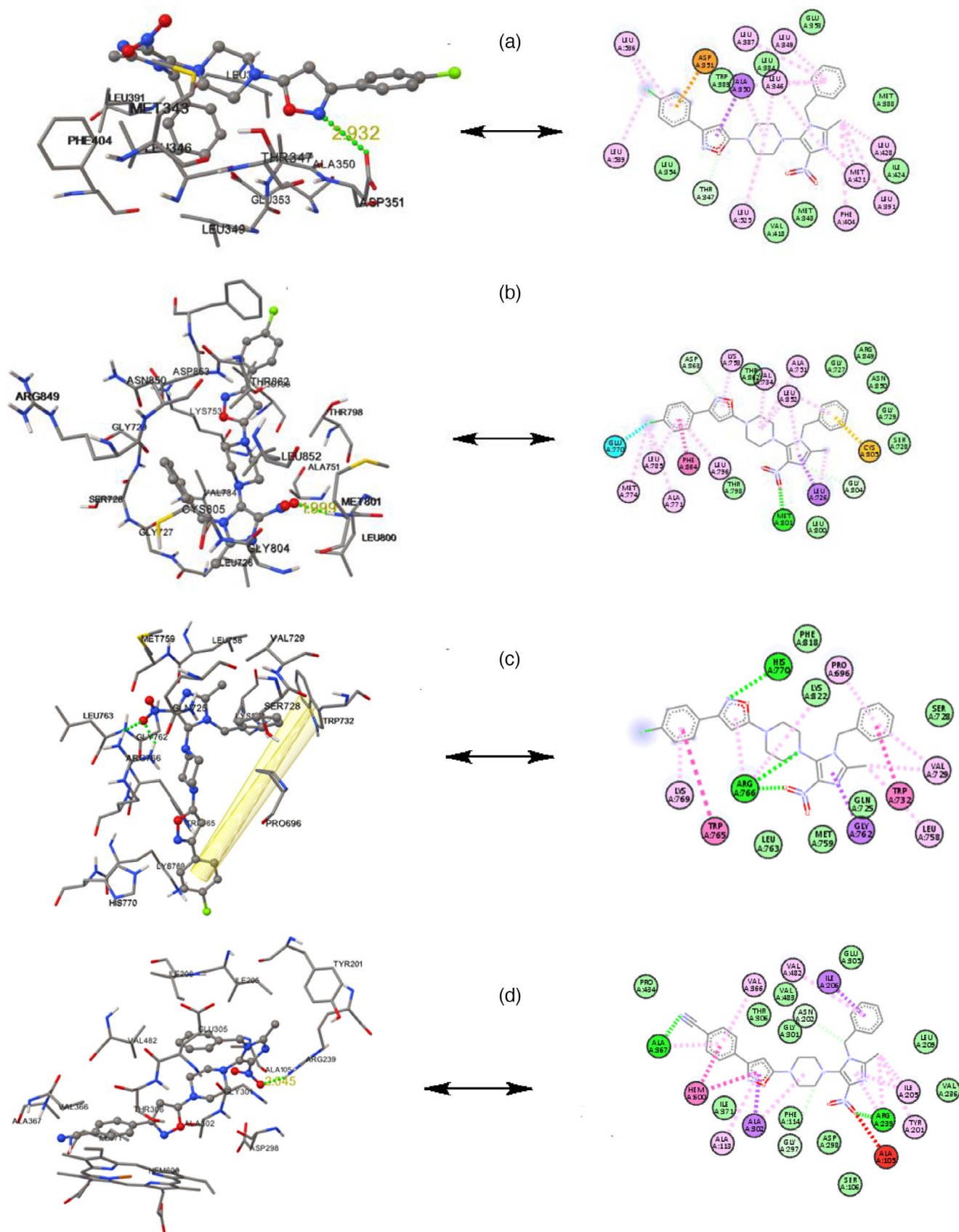


Figure 3. The binding modes of compound **9a** against breast cancer with (a): estrogen receptor (3ERT); (b): progesterone receptor (3G8O), and (c): HERT2 (3PP0) were generated from the crystal structures in PDB database as well as binding of compound **9j** against prostate cancer with (d): human androgen receptor (3E1G) and (e): human cytochrome P450 CYP17A1 (3RUK).

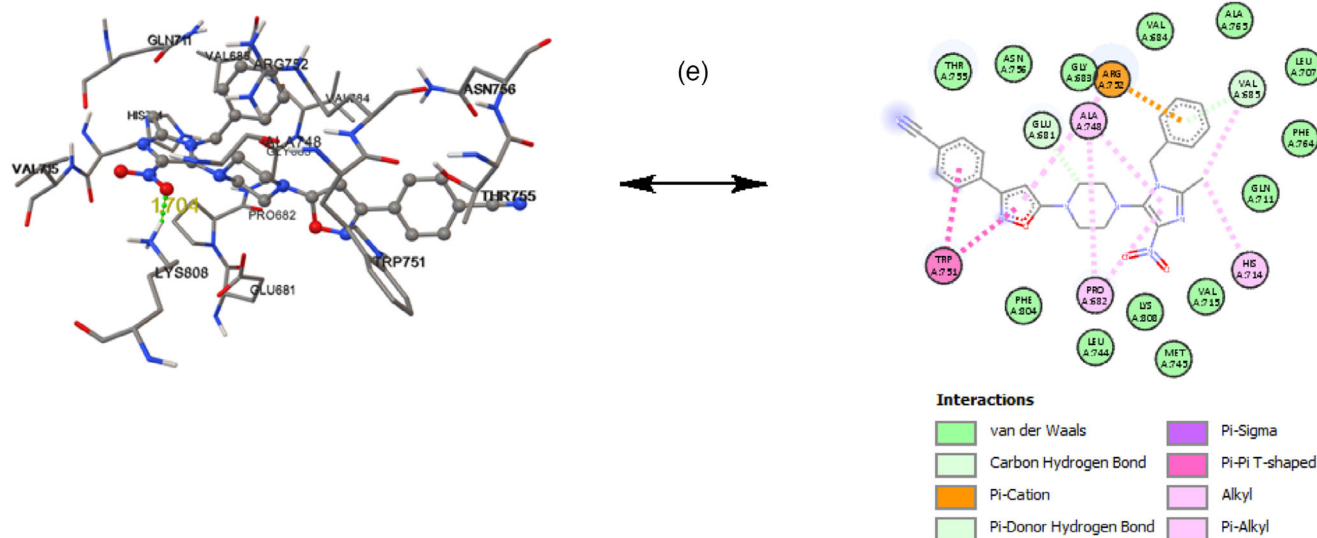


Figure 3. Continued

isoxazole moieties. Moreover, several non-bonded interactions, including σ - π , alkyl- π , π -cation, and π -anion interactions, surround compounds **9a** and **9j** were witnessed, potentially enhancing their inhibitory potency. Table 3 showed the docking results calculated with Autodock 4.6.

In summary, our refinement of structure-based hits led to the identification of inhibitors **9a** and **9j** against breast and prostate cancers, which target human ER, PR, HER2, and the human androgen receptor, respectively. These findings offer promising avenues for novel drug discovery focused on developing treatments for breast and prostate cancers.

4. Conclusions

In summary, we have developed a series of novel piperazine conjugated 3,5-disubstituted isoxazole analogs **9a-o**. The structures of these newly synthesized compounds were verified using spectral and mass analysis. Their anticancer activity was assessed against breast cancer cell lines (MCF-7 and MDA-MB-231) and prostate cancer cell lines (PC-3 and DU-145). Most of these compounds showed strong cytotoxic activity against MCF-7 and PC-3 cell lines. Compounds **9a**, **9j**, **9k**, and **9o** exhibited significant cytotoxic effects against MCF-7 cells with IC_{50} values (0.052–0.012 μ M), while compounds **9a**, **9d**, **9g**, **9j**, and **9k** dis-

played notable cytotoxicity against PC-3 cells with IC_{50} values (0.156 and 0.041 μ M). These results indicated that these molecules have strong potential for further development. Molecular docking studies showed that compound **9a** exhibited strong binding interactions with human protein receptors ER, PR, and HER2, while compound **9j** demonstrated significant binding affinity with the androgen receptor CYP450 17A1. Ongoing research is focused on expanding structural diversity, investigating mechanisms of action, and utilizing pharmacogenetic approaches to develop more effective therapeutic candidates.

5. Experimental

5.1. Materials and Methods

Melting points (m.p, uncorrected in $^{\circ}$ C) are determined on the electrothermal melting point apparatus and Stuart (SMP-10) melting point apparatus. The NMR spectra are recorded on a Bruker Avance III-(500 MHz) spectrometer with TMS as an internal standard. 1 H NMR (500 MHz), 13 C NMR (125 MHz) and 2D are recorded in deuterated chloroform ($CDCl_3$) or Dimethylsulfoxide ($DMSO-d_6$). Chemical shifts are expressed in δ units and are reported in ppm and J coupling values for 1 H- 1 H coupling constants are given in Hz. High-resolution mass spectra (HRMS) are measured (in positive / or negative ion mode) using the electrospray ion trap (ESI pos low mass) technique by collision-induced dissociation on a Bruker APEX-

Table 2. Docking results calculated with Autodock 4.6.

Compd. Protein	Binding Energy Kcal/mol	K_i (nM)	Intermolecular Energy	Internal Energy	Torsional Energy	Unbound Extended Energy	Hydrogen Bond(Å)
9a /3RET	−10.3	27.96	−10.43	−1.78	1.79	−0.11	Thr347:(O-isoxazole) = 2.932
9a /3PP0	−13.32	172.75	−13.40	−1.82	1.79	−0.11	Met801:NO ₂ = 1.991
9a /3G8O	−9.03	238.82	−9.69	−1.22	1.79	−0.11	Arg766:NO ₂ = 2.026 Arg766:NO ₂ = 1.734
9j /3RUK	−10.12	38.22	−10.65	−1.35	1.79	−0.11	Ala105:NO ₂ = 2.045
9j /1E3G	−8.17	1.03 (μ M)	−9.75	−0.30	1.79	−0.10	Lys808:NO ₂ = 1.704

IV (7 Tesla) instrument. The chemicals are purchased from Aldrich (Riedstraße, Germany), Fluka (Buchs, Switzerland), and Scharlau, are used without further purification, unless otherwise stated.

5.2. Chemistry

5.2.1. Preparation of 3, 5-Disubstituted Isoxazoles

General Procedure for the Synthesis of Substituted Benzaldehyde Oxime 7a-o: To a stirred solution of hydroxylamine hydrochloride (1.85 g, 26.6 mmol) and sodium acetate trihydrate (9.06 g, 66.6 mmol) in THF-EtOH-H₂O (30 mL:75 mL: 15 mL), the resulting solution was warmed about 40 °C, substituted benzaldehyde (3.0 g, 24.2 mmol) was added, the mixture was stirred at r.t. for 25 min. The mixture was cooled in an ice bath to complete precipitation. The residue was extracted with Et₂O, washed with brine, dried over sodium sulfate and filtered. The solvent was evaporated, the produced product was recrystallized from ethanol to give the desired product (3.36 g, 100%), which was used in the next step.

General Procedure for the Synthesis of Substituted-N-Hydroxybenzimidoyl Chloride 8a-o: A stirred solution of N-chlorosuccinimide NCS (3.55 g, 26.6 mmol) in DMF-CH₂Cl₂ (20 mL: 120 mL) was added drop wise to the solution of pyridine (200 µL, 2.42 mmol) and (7a-o) substituted benzaldehyde oxime (3.36 g, 24.2 mmol) in CH₂Cl₂ (120 mL). The solution was stirred at r.t. for 12 h, the reaction mixture was washed with H₂O (5 × 100 mL). The organic layer was separated, the aqueous phases were collected and extracted again with EtOAc (20 mL). The combined organic layers were dried (Na₂SO₄), filtered, and evaporated to dryness to afford 8a-o (4.2 g, 100%). The substituted-N-hydroxybenzimidoyl chloride was used in the next step without further purification.

5.2.2. General Procedure for the Synthesis of 5-((4-(N¹-benzyl-2-methyl-4-nitro-1H-imidazol-5-yl)piperazin-1-yl)methyl)-3-(substituted)isoxazole (9a-o)

A mixture of 1-(N¹-benzyl-2-methyl-4-nitro-1H-imidazol-5-yl)-4-(prop-2-yn-1-yl)piperazine (6) (0.5 g, 1.0 eq.) and CuI (1/10 = 0.1 eq.) was stirred in 10–15 mL of toluene. After stirring for 15–30 min, Et₃N (3.7 eq.) was added and the mixture was stirred for additional 15 min. The corresponding substituted-N-hydroxybenzimidoyl chloride 8a-o (1.3 eq.) was then added and the reaction mixture was stirred overnight, with progress by TLC. Chloroform (20 mL) was added to the reaction mixture, followed by filtration. The filtrate was washed with water (10–15 mL) and the organic phase was extracted and evaporated to dryness under vacuum. The product was purified using SiO₂ column chromatography using 5% EtOAc:n-hexane as the eluent, yielding the pure compounds.

5-((4-(N¹-benzyl-2-methyl-4-nitro-1H-imidazol-5-yl)piperazin-1-yl)methyl)-3-(4-chlorophenyl)isoxazole (9a). Light brown solid; Yield: 0.60 g (67%); M.p. = 96–98 °C; ¹H NMR (500 MHz, CDCl₃) δ: 2.27 (s, 3H, CH₃), 2.54 (br s., 4H, H_{piperazin-3''}+H_{piperazin-5''}), 3.31 (br s., 4H, H_{piperazin-2''}+H_{piperazin-6''}), 3.72 (s, 2H, CH₂C_{isoxazol-5''}), 5.05 (s, 2H, NCH₂Ph), 6.47 (s, 2H, H_{isoxazol-4''}), 6.96 (d, J = 7.3 Hz, 2H, H_{arom.-2'}+H_{arom.-6'}), 7.23–7.32 (m, 3H, H_{arom.}), 7.39 (d, J = 7.9 Hz, 2H, H_{arom.-3'''}+H_{arom.-5'''}), 7.72 (d, J = 8.7 Hz, 2H, H_{arom.-2'''}+H_{arom.-6'''}); ¹³C NMR (125 MHz, CDCl₃) δ: 14.1 (CH₃), 46.4 (NCH₂Ph), 49.1 (C_{piperazin-2''}+C_{piperazin-6''}), 52.6 (C_{piperazin-3''}+C_{piperazin-5''}), 53.1 (CH₂C_{isoxazol-5''}), 101.2 (C_{isoxazol-4''}), 125.9–139.0 (C_{arom.}), 136.1 (C–Cl), 138.3 (C–NO₂), 139.5 (C-5), 140.6 (C-2), 161.5 (C_{isoxazol-5''}), 170.2 (C_{isoxazol-3''}); HRMS (ESI)

m/z: Calculated for C₂₅H₂₅ClN₆O₃Na = 515.15689, found 515.15772 [M + Na]⁺.

5-((4-(N¹-benzyl-2-methyl-4-nitro-1H-imidazol-5-yl)piperazin-1-yl)methyl)-3-(p-tolyl) isoxazole (9b). Caramel solid; Yield: 0.50 g (68%); Mp = 84–86 °C; ¹H NMR (500 MHz, CDCl₃) δ: 2.25 (s, 3H, CH₃), 2.37 (s, 3H, CH₃Ar), 2.56 (br s., 4H, H_{piperazin-3''}+H_{piperazin-5''}), 3.08 (br s., 4H, H_{piperazin-2''}+H_{piperazin-6''}), 3.74 (s, 2H, CH₂C_{isoxazol-5''}), 5.05 (s, 2H, NCH₂Ph), 6.48 (s, 1H, H_{isoxazol-4''}), 6.94 (d, J = 6.9 Hz, 2H, H_{arom.-2'}+H_{arom.-6'}), 7.23 (t, J = 7.3 Hz, 1H, H_{arom.-4'}), 7.28–7.32 (m, 2H, H_{arom.-3'}+H_{arom.-5'}), 7.67 (m, 2H, H_{arom.-3'''}+H_{arom.-5'''}), 7.94 (d, J = 7.9 Hz, 2H, H_{arom.-2'''}+H_{arom.-6'''}); ¹³C NMR (125 MHz, CDCl₃) δ: 14.3 (CH₃), 21.4 (CH₃Ar), 46.5 (NCH₂Ph), 48.9 (C_{piperazin-2''}+C_{piperazin-6''}), 52.9 (C_{piperazin-3''}+C_{piperazin-5''}), 53.3 (CH₂C_{isoxazol-5''}), 101.5 (C_{isoxazol-4''}), 125.8–140.2 (C_{arom.}), 142.6 (C-5), 143.8 (C-2), 162.4 (C_{isoxazol-5''}), 169.7 (C_{isoxazol-3''}); HRMS (ESI) m/z: Calculated for C₂₆H₂₈N₆O₃Na = 495.21151, found 495.21280 [M + Na]⁺.

5-((4-(N¹-benzyl-2-methyl-4-nitro-1H-imidazol-5-yl)piperazin-1-yl)methyl)-3-(2-methoxyphenyl)isoxazole (9c). Cumin solid; Yield: 0.20 g (83%); Mp = 89–91 °C; ¹H NMR (500 MHz, CDCl₃) δ: 2.26 (s, 3H, CH₃), 2.55 (br s., 4H, H_{piperazin-3''}+H_{piperazin-5''}), 3.08 (br s., 4H, H_{piperazin-2''}+H_{piperazin-6''}), 3.73 (s, 3H, OCH₃), 3.86 (s, 2H, CH₂C_{isoxazol-5''}), 5.05 (s, 2H, NCH₂Ph), 6.67 (s, 1H, H_{isoxazol-4''}), 6.89 (d, J = 8.9 Hz, 1H, H_{arom.-3'''}), 6.95 (d, J = 6.9 Hz, 2H, H_{arom.-2'}+H_{arom.-6'}), 7.01 (m, 1H, H_{arom.-5'''}), 7.23–7.32 (m, 3H, H_{arom.-3'}+H_{arom.-4'}+H_{arom.-5'}), 7.36 (m, 1H, H_{arom.-4'''}), 7.85 (br s., 1H, H_{arom.-6'''}); ¹³C NMR (125 MHz, CDCl₃) δ: 14.1 (CH₃), 46.5 (NCH₂Ph), 49.1 (C_{piperazin-2''}+C_{piperazin-6''}), 53.0 (C_{piperazin-3''}+C_{piperazin-5''}), 53.4 (CH₂C_{isoxazol-5''}), 55.9 (OCH₃), 104.7 (C_{isoxazol-4''}), 112.8 (C_{isoxazol-3''}), 119.3 (C_{arom.-1'''}), 120.9 (C_{arom.-5'''}), 125.9–135.2 (C_{arom.}), 139.4 (C-4), 139.7 (C-5), 140.1 (C-2), 155.8 (C_{arom.-2'''}), 157.2 (C_{isoxazol-5''}), 168.8 (C_{isoxazol-3''}); HRMS (ESI) m/z: Calculated for C₂₆H₂₈N₆O₄Na = 511.20642, found 511.20556 [M + Na]⁺, Calculated for C₂₆H₂₉N₆O₄ = 489.22448, found 489.22411 [M + H]⁺.

5-((4-(N¹-benzyl-2-methyl-4-nitro-1H-imidazol-5-yl)piperazin-1-yl)methyl)-3-(4-nitrophenyl)isoxazole (9d). Turmeric solid; Yield: 0.20 g (81%); Mp = 118–120 °C; ¹H NMR (500 MHz, CDCl₃) δ: 2.27 (s, 3H, CH₃), 2.59 (br s., 4H, H_{piperazin-3''}+H_{piperazin-5''}), 3.16 (br s., 4H, H_{piperazin-2''}+H_{piperazin-6''}), 3.59 (s, 2H, CH₂C_{isoxazol-5''}), 5.06 (s, 2H, NCH₂Ph), 6.61 (s, 1H, H_{isoxazol-4''}), 6.96 (d, J = 7.1 Hz, 2H, H_{arom.-2'}+H_{arom.-6'}), 7.23–7.32 (m, 3H, H_{arom.-3'}+H_{arom.-5'}+H_{arom.-4'}), 7.97 (d, J = 8.5 Hz, 2H, H_{arom.-2'''}+H_{arom.-6'''}), 8.28 (d, J = 8.5 Hz, 2H, H_{arom.-3'''}+H_{arom.-5'''}); ¹³C NMR (125 MHz, CDCl₃) δ: 14.1 (CH₃), 46.6 (NCH₂Ph), 48.9 (C_{piperazin-2''}+C_{piperazin-6''}), 52.4 (C_{piperazin-3''}+C_{piperazin-5''}), 53.3 (CH₂C_{isoxazol-5''}), 101.6 (C_{isoxazol-4''}), 123.9–136.9 (C_{arom.}), 138.4 (C-4), 138.8 (C-5), 143.2 (C-2), 148.7 (CNO₂), 160.7 (C_{isoxazol-5''}), 170.9 (C_{isoxazol-3''}); HRMS (ESI) m/z: Calculated for C₂₅H₂₅N₇O₅Na = 526.18094, found 526.18281 [M + Na]⁺.

5-((4-(N¹-benzyl-2-methyl-4-nitro-1H-imidazol-5-yl)piperazin-1-yl)methyl)-3-(o-tolyl) isoxazole (9e). Light-brown solid; Yield: 0.20 g (74%); Mp = 106–108 °C; ¹H NMR (500 MHz, CDCl₃) δ: 2.27 (s, 3H, CH₃), 2.44 (s, 3H, CH₃C_{arom.-2'''}), 2.61 (br s., 4H, H_{piperazin-3''}+H_{piperazin-5''}), 3.15 (br s., 4H, H_{piperazin-2''}+H_{piperazin-6''}), 3.75 (s, 2H, CH₂C_{isoxazol-5''}), 5.05 (s, 2H, NCH₂Ph), 6.36 (s, 1H, H_{isoxazol-4''}), 6.96 (d, J = 6.7 Hz, 2H, H_{arom.-2'}+H_{arom.-6'}), 7.23–7.32 (m, 5H, H_{arom.-3'}+H_{arom.-4'}+H_{arom.-5'}+H_{arom.-4'''}+H_{arom.-5'''}), 7.36 (d, J = 7.6 Hz, 1H, H_{arom.-3'''}), 7.45 (d, J = 7.1 Hz, 1H, H_{arom.-6'''}); ¹³C NMR (125 MHz, CDCl₃) δ: 14.1 (CH₃), 21.1 (CH₃C_{arom.-2'''}), 46.5 (NCH₂Ph), 49.1 (C_{piperazin-2''}+C_{piperazin-6''}), 52.6 (C_{piperazin-3''}+C_{piperazin-5''}), 53.4 (CH₂C_{isoxazol-5''}), 104.0 (C_{isoxazol-4''}), 125.7–136.8 (C_{arom.}), 139.2 (C-4), 139.6 (C-5), 140.2 (C-2), 163.1 (C_{isoxazol-5''}), 168.8 (C_{isoxazol-3''}); HRMS (ESI) m/z: Calculated for C₂₆H₂₈N₆O₃Na = 495.21151, found 495.21341 [M + Na]⁺.

5-((4-(N¹-benzyl-2-methyl-4-nitro-1H-imidazol-5-yl)piperazin-1-yl)methyl)-3-(2-chlorophenyl)isoxazole (9f). Pale-yellow solid; Yield: 0.30 g (51%); Mp = 62–64 °C; ¹H NMR (500 MHz, CDCl₃) δ: 2.29 (s, 3H, CH₃), 2.63 (br s., 4H, H_{piperazin-3''}+H_{piperazin-5''}), 3.06 (br s., 4H, H_{piperazin-2''}+H_{piperazin-6''}), 3.82 (s, 2H, CH₂C_{isoxazol-5''}), 5.05

(s, 2H, NCH₂Ph), 6.69 (s, 1H, H_{isoxazol-4}'''), 6.96 (d, *J* = 7.2 Hz, 2H, H_{arom.-2'}+H_{arom.-6'}), 7.23–7.37 (m, 5H, H_{arom.-3'} + H_{arom.-4'} + H_{arom.-5'}+H_{arom.-4}'''+H_{arom.-5}'''), 7.46 (d, *J* = 7.4 Hz, 1H, H_{arom.-3}'''), 7.69 (d, *J* = 7.5 Hz, 1H, H_{arom.-6}'''); ¹³C NMR (125 MHz, CDCl₃) δ: 14.1 (CH₃), 46.5 (NCH₂Ph), 49.1 (C_{piperazin-2'}+C_{piperazin-6'}), 52.6 (C_{piperazin-3'}+C_{piperazin-5'}), 56.1 (CH₂C_{isoxazol-5}'''), 102.2 (C_{isoxazol-4}'''), 125.7–136.8 (C_{arom.}), 132.2 (C_{icarom.-2}'''), 139.2 (C-4), 139.6 (C-5), 140.2 (C-2), 158.9 (C_{isoxazol-5}'''), 162.8 (C_{isoxazol-3}'''); HRMS (ESI) *m/z*: Calculated for C₂₅H₂₅ClN₆O₃Na = 515.15689, found 151.1740 [M + Na]⁺. Calculated for C₂₅H₂₆ClN₆O₃ = 493.17494, found 493.17557 [M + H]⁺.

5-((4-(N¹-benzyl-2-methyl-4-nitro-1H-imidazol-5-yl)piperazin-1-yl)methyl)-3-(3-bromophenyl)isoxazole (9g). Beige solid; Yield: 0.15 g (48%); Mp = 109–111 °C; ¹H NMR (500 MHz, CDCl₃) δ: 2.27 (s, 3H, CH₃), 2.63 (br s., 4H, H_{piperazin-3'}+H_{piperazin-5'}), 3.32 (br s., 4H, H_{piperazin-2'}+H_{piperazin-6'}), 3.74 (s, 2H, CH₂C_{isoxazol-5}'''), 5.05 (s, 2H, NCH₂Ph), 6.46 (s, 1H, H_{isoxazol-4}'''), 6.96 (d, *J* = 7.4 Hz, 2H, H_{arom.-2'}+H_{arom.-6'}), 7.23–7.35 (m, 4H, H_{arom.-3'}+H_{arom.-5'}+H_{arom.-4'}+H_{arom.-5}'''), 7.53 (d, *J* = 7.8 Hz, 1H, H_{arom.-4}'''), 7.71 (d, *J* = 7.6 Hz, H_{arom.-6}'''), 7.92 (s, 1H, H_{arom.-2}'''); ¹³C NMR (125 MHz, CDCl₃) δ: 14.1 (CH₃), 46.6 (NCH₂Ph), 49.1 (C_{piperazin-2'}+C_{piperazin-6'}), 52.6 (C_{piperazin-3'}+C_{piperazin-5'}), 53.2 (CH₂C_{isoxazol-5}'''), 101.4 (C_{isoxazol-4}'''), 122.9 (C_{arom.-3}'''), 125.9–135.2 (C_{arom.}), 139.0 (C-4), 139.4 (C-5), 140.2 (C-2), 161.2 (C_{isoxazol-5}'''), 170.3 (C_{isoxazol-3}'''); HRMS (ESI) *m/z*: Calculated for C₂₅H₂₅BrN₆O₃Na = 559.10637: 561.11290, found 559.10615: 561.11290 [M + Na]⁺.

5-((4-(N¹-benzyl-2-methyl-4-nitro-1H-imidazol-5-yl)piperazin-1-yl)methyl)-3-(4-methoxyphenyl)isoxazole (9 h). Off-white solid; Yield: 0.15 g (84%); Mp = 158–160 °C; ¹H NMR (500 MHz, CDCl₃) δ: 2.27 (s, 3H, CH₃), 2.62 (br s., 4H, H_{piperazin-3'}+H_{piperazin-5'}), 3.05 (br s., 4H, H_{piperazin-2'}+H_{piperazin-6'}), 3.30 (s, 2H, CH₂C_{isoxazol-5}'''), 3.81 (s, 3H, OCH₃), 5.04 (s, 2H, NCH₂Ph), 6.41 (s, 1H, H_{isoxazol-4}'''), 6.94 (d, *J* = 8.9 Hz, 2H, H_{arom.-2'}+H_{arom.-6'}), 7.23–7.32 (m, 3H, H_{arom.-3'}+H_{arom.-4'}+H_{arom.-5'}), 7.64 (m, 2H, H_{arom.-3}'''+H_{arom.-5}'''), 7.70 (d, *J* = 8.5 Hz, 2H, H_{arom.-2}'''+H_{arom.-6}'''); ¹³C NMR (125 MHz, CDCl₃) δ: 14.1 (CH₃), 46.7 (NCH₂Ph), 49.1 (C_{piperazin-2'}+C_{piperazin-6'}), 53.2 (C_{piperazin-3'}+C_{piperazin-5'}), 53.4 (CH₂C_{isoxazol-5}'''), 56.3 (OCH₃), 101.1 (C_{isoxazol-4}'''), 114.3 (C_{arom.-3}'''+C_{arom.-5}'''), 123.1–135.2 (C_{arom.}), 139.2 (C-4), 139.4 (C-5), 143.2 (C-2), 156.3 (C_{isoxazol-5}'''), 161.0 (C_{arom.-4}'''), 170.0 (C_{isoxazol-3}'''); HRMS (ESI) *m/z*: Calculated for C₂₆H₂₈N₆O₄Na = 511.20642, found 511.20778 [M + Na]⁺.

5-((4-(N¹-benzyl-2-methyl-4-nitro-1H-imidazol-5-yl)piperazin-1-yl)methyl)-3-(2-chloro-5-nitrophenyl) isoxazole (9i). Dark-yellow solid; Yield: 0.15 g (62%); Mp = 113–115 °C; ¹H NMR (500 MHz, CDCl₃) δ: 2.27 (s, 3H, CH₃), 2.65 (br s., 4H, H_{piperazin-3'}+H_{piperazin-5'}), 3.31 (br s., 4H, H_{piperazin-2'}+H_{piperazin-6'}), 3.78 (s, 2H, CH₂C_{isoxazol-5}'''), 5.07 (s, 2H, NCH₂Ph), 6.68 (s, 1H, H_{isoxazol-4}'''), 6.98 (d, *J* = 7.5 Hz, 2H, H_{arom.-2'}+H_{arom.-6'}), 7.23–7.33 (m, 3H, H_{arom.-3'}+H_{arom.-4'}+H_{arom.-5'}), 7.66 (d, *J* = 8.7 Hz, 1H, H_{arom.-3}'''), 8.21 (d, *J* = 8.7 Hz, 1H, H_{arom.-4}'''), 8.59 (s, 1H, H_{arom.-6}'''); ¹³C NMR (125 MHz, CDCl₃) δ: 14.1 (CH₃), 46.7 (NCH₂Ph), 49.1 (C_{piperazin-2'}+C_{piperazin-6'}), 53.2 (C_{piperazin-3'}+C_{piperazin-5'}), 53.4 (CH₂C_{isoxazol-5}'''), 104.3 (C_{isoxazol-4}'''), 125.2–135.2 (C_{arom.}), 138.9 (C_{arom.-2}'''), 139.4 (C-4), 139.6 (C-5), 140.4 (C-2), 146.6 (C_{arom.-5}'''), 159.4 (C_{isoxazol-5}'''), 170.1 (C_{isoxazol-3}'''); HRMS (ESI) *m/z*: Calculated for C₂₅H₂₄ClN₇O₅Na = 560.14197, found 560.14285 [M + Na]⁺.

4-5-((4-(N¹-benzyl-2-methyl-4-nitro-1H-imidazol-5-yl)piperazin-1-yl)methyl) isoxazol-3-yl) benzonitrile (9j). Yellow solid; Yield: 0.15 g (77%); Mp = 77–79 °C; ¹H NMR (500 MHz, CDCl₃) δ: 2.27 (s, 3H, CH₃), 2.55 (br s., 4H, H_{piperazin-3'}+H_{piperazin-5'}), 3.32 (br s., 4H, H_{piperazin-2'}+H_{piperazin-6'}), 3.77 (s, 2H, CH₂C_{isoxazol-5}'''), 5.07 (s, 2H, NCH₂Ph), 6.52 (s, 1H, H-4'''), 6.96 (d, *J* = 7.3 Hz, 2H, H-2'+H-6'), 7.23–7.34 (m, 3H, H_{arom.-3'}+H_{arom.-5'}+H_{arom.-4'}), 7.71 (d, *J* = 6.2 Hz, 2H, H_{arom.-2}'''+H_{arom.-6}'''), 7.88 (d, *J* = 6.7 Hz, 2H, H_{arom.-3}'''+H_{arom.-5}'''); ¹³C NMR (125 MHz, CDCl₃) δ: 14.1 (CH₃), 46.5 (NCH₂Ph), 48.9 (C_{piperazin-2'}+C_{piperazin-6'}), 52.6 (C_{piperazin-3'}+C_{piperazin-5'}), 53.2 (CH₂C_{isoxazol-5}'''),

101.5 (C_{isoxazol-4}'''), 113.6 (C_{arom.-4}'''), 118.3 (CN), 125.9–135.2 (C_{arom.}), 139.4 (C-4), 139.5 (C-5), 140.6 (C-2), 160.9 (C_{isoxazol-5}'''), 171.0 (C_{isoxazol-3}'''); HRMS (ESI) *m/z*: Calculated for C₂₆H₂₅N₇O₃Na = 506.19111, found 506.19027 [M + Na]⁺.

4-5-((4-(N¹-benzyl-2-methyl-4-nitro-1H-imidazol-5-yl)piperazin-1-yl)methyl)isoxazol-3-yl)-N,N-dimethylaniline (9k). Off-white solid; Yield: 0.15 g (84%); Mp = 92–94 °C; ¹H NMR (500 MHz, CDCl₃) δ: 2.27 (s, 3H, CH₃), 2.71 (br s., 4H, H_{piperazin-3'}+H_{piperazin-5'}), 2.85 (s, 6H, CH₃NCH₃), 3.36 (br s., 4H, H_{piperazin-2'}+H_{piperazin-6'}), 3.72 (s, 2H, CH₂C_{isoxazol-5}'''), 5.05 (s, 2H, NCH₂Ph), 6.43 (s, 1H, H_{isoxazol-4}'''), 6.95 (d, *J* = 7.0 Hz, 2H, H_{arom.-2'}+H_{arom.-6'}), 7.23–7.34 (m, 3H, H_{arom.-3'}+H_{arom.-5'}+H_{arom.-4'}), 7.06 (d, *J* = 8.4 Hz, 2H, H_{arom.-3}'''+H_{arom.-5}'''), 7.61 (d, *J* = 8.3 Hz, 2H, H_{arom.-2}'''+H_{arom.-6}'''); ¹³C NMR (125 MHz, CDCl₃) δ: 14.1 (CH₃), 43.3 (CH₃NCH₃), 46.6 (NCH₂Ph), 49.1 (C_{piperazin-2'}+C_{piperazin-6'}), 52.6 (C_{piperazin-3'}+C_{piperazin-5'}), 53.0 (CH₂C_{isoxazol-5}'''), 101.1 (C_{isoxazol-4}'''), 119.9 (C_{arom.-3}'''+C_{arom.-5}'''), 123.5 (C_{arom.-1}'''), 125.9–135.2 (C_{arom.}), 139.0 (C-4), 139.4 (C-5), 140.6 (C-2), 151.8 (C_{arom.-4}'''), 161.2 (C_{isoxazol-5}'''), 169.8 (C_{isoxazol-3}'''); HRMS (ESI) *m/z*: Calculated for C₂₆H₂₅N₇O₃Na = 524.20711, found 524.20611 [M + Na]⁺.

5-((4-(N¹-benzyl-2-methyl-4-nitro-1H-imidazol-5-yl)piperazin-1-yl)methyl)-3-phenylisoxazole (9l). Off-white solid; Yield: 0.15 g (60.7%); Mp = 74–76 °C; ¹H NMR (500 MHz, CDCl₃) δ: 2.20 (s, 3H, CH₃), 2.95 (br s., 4H, H_{piperazin-3'}+H_{piperazin-5'}), 3.69 (br s., 4H, H_{piperazin-2'}+H_{piperazin-6'}), 4.07 (s, 2H, CH₂C_{isoxazol-5}'''), 5.11 (s, 2H, NCH₂Ph), 7.03 (s, 1H, H_{arom.-4}'''), 7.23 (br s., 2H, H_{arom.-2'}+H_{arom.-6'}), 7.31 (m, 3H, H_{arom.-3'}+H_{arom.-5'}+H_{arom.-4'}), 7.43 (br s., 3H, H_{arom.-3}'''+H_{arom.-4}'''+H_{arom.-5}'''), 7.78 (br s., 2H, H_{arom.-2}'''+H_{arom.-6}'''); ¹³C NMR (125 MHz, CDCl₃) δ: 14.3 (CH₃), 46.5 (NCH₂Ph), 48.9 (C_{piperazin-2'}+C_{piperazin-6'}), 52.9 (C_{piperazin-3'}+C_{piperazin-5'}), 53.3 (CH₂C_{isoxazol-5}'''), 125.8–140.2 (C_{arom.}), 142.6 (C-5), 143.8 (C-2), 162.4 (C_{isoxazol-5}'''), 169.7 (C_{isoxazol-3}'''); HRMS (ESI) *m/z*: Calculated for C₂₅H₂₆N₆O₃Na = 481.19586, found 481.19399 [M + Na]⁺.

5-((4-(N¹-benzyl-2-methyl-4-nitro-1H-imidazol-5-yl)piperazin-1-yl)methyl)-3-(4-bromophenyl)isoxazole (9m). Yellow solid; Yield: 0.15 g (97%); Mp = 94–96 °C; ¹H NMR (500 MHz, CDCl₃) δ: 2.27 (s, 3H, CH₃), 2.55 (br s., 4H, H_{piperazin-3'}+H_{piperazin-5'}), 3.07 (br s., 4H, H_{piperazin-2'}+H_{piperazin-6'}), 3.73 (s, 2H, CH₂C_{isoxazol-5}'''), 5.05 (s, 2H, NCH₂Ph), 6.48 (s, 1H, H-4'''), 6.95 (d, *J* = 7.2 Hz, 2H, H-2'+H-6'), 7.27–7.31 (m, 3H, H_{arom.-3'}+H_{arom.-5'}+H_{arom.-4'}), 7.57 (d, *J* = 7.9 Hz, 2H, H_{arom.-3}'''+H_{arom.-5}'''), 7.66 (d, *J* = 8.3 Hz, 2H, H_{arom.-2}'''+H_{arom.-6}'''); ¹³C NMR (125 MHz, CDCl₃) δ: 14.1 (CH₃), 46.4 (NCH₂Ph), 49.1 (C_{piperazin-2'}+C_{piperazin-6'}), 53.1 (C_{piperazin-3'}+C_{piperazin-5'}), 53.4 (CH₂C_{isoxazol-5}'''), 101.2 (C_{isoxazol-4}'''), 124.3 (CBr), 125.9–135.2 (C_{arom.}), 139.2 (C-4), 139.5 (C-5), 140.0 (C-2), 161.5 (C_{isoxazol-5}'''), 170.3 (C_{isoxazol-3}'''); HRMS (ESI) *m/z*: Calculated for C₂₅H₂₅BrN₆O₃Na = 559.10637: 561.10469, found 559.10594: 561.10658 [M + Na]⁺.

5-((4-(N¹-benzyl-2-methyl-4-nitro-1H-imidazol-5-yl)piperazin-1-yl)methyl)-3-(4-fluorophenyl)isoxazole (9n). Ivory solid; Yield: 0.15 g (94%); Mp = 63–65 °C; ¹H NMR (500 MHz, CDCl₃) δ: 2.28 (s, 3H, CH₃), 2.67 (br s., 4H, H_{piperazin-3'}+H_{piperazin-5'}), 3.41 (br s., 4H, H_{piperazin-2'}+H_{piperazin-6'}), 3.77 (s, 2H, CH₂C_{isoxazol-5}'''), 5.05 (s, 2H, NCH₂Ph), 6.50 (s, 1H, H_{isoxazol-4}'''), 6.96 (d, *J* = 7.2 Hz, 2H, H_{arom.-2'}+H_{arom.-6'}), 7.12 (d, *J* = 8.4 Hz, 2H, H_{arom.-3}'''+H_{arom.-5}'''), 7.23–7.33 (m, 3H, H_{arom.-3'}+H_{arom.-5'}+H_{arom.-4'}), 7.77 (d, *J* = 8.0 Hz, 2H, H_{arom.-2}'''+H_{arom.-6}'''); ¹³C NMR (125 MHz, CDCl₃) δ: 14.1 (CH₃), 46.4 (NCH₂Ph), 49.1 (C_{piperazin-2'}+C_{piperazin-6'}), 53.1 (C_{piperazin-3'}+C_{piperazin-5'}), 53.4 (CH₂C_{isoxazol-5}'''), 101.2 (C_{isoxazol-4}'''), 125.9–135.2 (C_{arom.}), 139.2 (C-4), 139.5 (C-5), 140.0 (C-2), 161.5 (C_{isoxazol-5}'''), 164.9 (CF), 170.3 (C_{isoxazol-3}'''); HRMS (ESI) *m/z*: Calculated for C₂₅H₂₅FN₆O₃Na = 499.18644, found 499.18745 [M + Na]⁺, calculated for C₂₅H₂₆FN₆O₃ = 477.20449, found 477.20507 [M + H]⁺.

5-((4-(1-benzyl-2-methyl-4-nitro-1H-imidazol-5-yl)piperazin-1-yl)methyl)-3-styrylisoxazole (9o). Pale-grey solid; Yield: 0.15 g (85%); Mp = 86–88 °C; ¹H NMR (500 MHz, CDCl₃) δ: 2.28 (s, 3H, CH₃), 2.57 (br s., 4H, H_{piperazin-3'}+H_{piperazin-5'}), 3.33 (br s.,

4H, $H_{\text{piperazin-2''}} + H_{\text{piperazin-6''}}$), 3.71 (s, 2H, $\text{CH}_2\text{C}_{\text{soxazol-5''}}$), 5.07 (s, 2H, NCH_2Ph), 6.44 (s, 1H, $H_{\text{soxazol-4''}}$), 6.96 (d, $J = 6.8$ Hz, 2H, $H_{\text{arom.-2'}} + H_{\text{arom.-6'}}$), 6.98 (d, $J_{\text{trans}} = 16.7$, 1H, $\text{CHC}_{\text{isoxazol-1''}}$), 7.14 (d, $J_{\text{trans}} = 16.6$, 1H, $\text{CHC}_{\text{soxazol-3''}}$), 7.29–7.36 (m, 6H, $H_{\text{arom.-3'}} + H_{\text{arom.-5'}} + H_{\text{arom.-4''}} + H_{\text{arom.-6''}} + H_{\text{arom.-5''}}$), 7.51 (d, $J = 7.3$ Hz, 2H, $H_{\text{arom.-2''}} + H_{\text{arom.-6''}}$); ^{13}C NMR (125 MHz, CDCl_3) δ : 14.1 (CH_3), 46.4 (NCH_2Ph), 49.1 ($\text{C}_{\text{piperazin-2''}} + \text{C}_{\text{piperazin-6''}}$), 53.1 ($\text{C}_{\text{piperazin-3''}} + \text{C}_{\text{piperazin-5''}}$), 53.4 ($\text{CH}_2\text{C}_{\text{soxazol-5''}}$), 101.2 ($\text{C}_{\text{soxazol-4''}}$), 114 ($\text{CHC}_{\text{soxazol-3''}}$), 125.9–135.2 ($\text{C}_{\text{arom.}}$), 136.6 ($\text{CH}=\text{CHC}_{\text{soxazol-3''}}$), 139.2 (C-4), 139.5 (C-5), 140.0 (C-2), 158.59 ($\text{C}_{\text{soxazol-5''}}$), 162.5 ($\text{C}_{\text{soxazol-3''}}$); HRMS (ESI) m/z : Calculated for $\text{C}_{27}\text{H}_{28}\text{N}_6\text{O}_3\text{Na} = 507.21151$, found 507.21157 [$\text{M} + \text{Na}$] $^+$, Calculated for $\text{C}_{27}\text{H}_{29}\text{N}_6\text{O}_3 = 485.22957$, found 485.22984 [$\text{M} + \text{H}$] $^+$.

5.3. Biological Assays

5.3.1. Cell Lines and Culture Conditions

Human breast adenocarcinoma (MCF-7, HTB-22), epithelial breast cancer (MDA-MB-231), androgen-resistant prostate cancer (PC-3), and androgen-sensitive prostate cancer (DU-145) cell lines were obtained from the American Type Culture Collection (ATCC, Rockville, MD, USA). MCF-7 cells were cultured in DMEM, while PC-3 and DU-145 cells were maintained in RPMI-1640 medium. The media were supplemented with 10% heat-inactivated fetal bovine serum (FBS), 1% (v/v) penicillin (10,000 units/mL)-streptomycin (10 mg/mL), and 1% (v/v) L-glutamine (200 mM) (all from Sigma-Aldrich). All cell lines were incubated at 37 °C in a fully humidified atmosphere with 5% CO_2 .

5.3.2. Cytotoxicity Assay

Cell lines were seeded into 96-well flat-bottom microplates with 100 μL of culture medium at the following densities: 3×10^3 cells per well for MCF-7, PC-3, MDA-MB-231, and DU-145. After allowing the cells to adhere for 24 h, the medium was replaced with either fresh medium alone or medium containing the tested compounds at increasing concentrations ranging from 0 to 250 μM for the cancer cell lines, and up to 500 μM for normal dermal fibroblasts. Paclitaxel (0–100 μM) and docetaxel (0–10 μM) were used as positive controls for growth inhibition. After 72 h of treatment, cell viability was assessed using the MTT assay (3-(4,5-dimethylthiazol-2-yl)-2,5-diphenyltetrazolium bromide).^[42] All experimental conditions were tested in triplicate, and the experiment was repeated three times. Half-maximal inhibitory concentrations (IC_{50}), representing the concentration needed for 50% inhibition of cell growth in vitro, were calculated using GraphPad Prism software (Version 8, San Diego, CA, USA), and the IC_{50} values are presented as mean \pm SD.

5.3.3. Statistical Analysis of Determination of Cytotoxicity and IC_{50} Values

Cellular cytotoxicity was quantified by normalizing absorbance values to those of untreated control cells, serving as the negative control. The percentage of cytotoxicity was calculated using the following formula, after background correction of absorbance readings:

$$\{\% \text{ Cytotoxicity}\} = 1 - \left(\frac{\text{Absorbance of experimental well}}{\text{Absorbance of negative control well}} \right) \times 100\%$$

The half maximal inhibitory concentration (IC_{50}) was determined by extrapolating from the generated dose-response curves. This value, representing the compound concentration at which cell viability was reduced by 50%, was calculated through regression analysis of triplicate data points across a range of concentrations using GraphPad PRISM software. The relative potency of the tested compounds was assessed via Parallel Line Assay (PLA version 1.2.06). All confidence limits and significance testing were established at a statistical threshold of $p < 0.05$.

5.3.4. Dock and Virtual Screening

Preparation of ligands and proteins: The structures of ligands **9a** and **9j** were generated using Avogadro software (v.1.0.1)^[45] and saved in PDB format. These ligand structures were then prepared by selecting torsions and converted from PDB to PDBQT format. The PDBQT files for both proteins and ligands, along with united atom Kollman charges, fragmental volumes, and solvation parameters, were generated using MGLTools software. Ligand structures were energy minimized using the MMFF94 force field. Before docking, native ligands and crystallographic water molecules were removed from the PDB structures, and polar hydrogens were added.

Author Contributions

Sadeekah Saber: Conceived and designed the experiments; Performed the Experiments; Analyzed and interpreted the data; Wrote the paper. Read AL-Qawasmeh and Yaseen Al-Soud: Conceived and designed the experiments. Najim A. Al-Masoudi: Analyzed and interpreted the data; Wrote the paper. Luay Abu-Qatouseh and Bahjat Saeed: Analyzed and interpreted the data; Contributed reagents, materials; Analysis tools or data.

Acknowledgments

The authors wish to thanks Deanship of Scientific Research at the University of Jordan and Al al-Bayt University for their support. RAA thanks office of vice chancellor for research and graduate studies for funded Project 23021440137. SOS thanks Prof. Muhammad I. Choudhary during a scientific visit to his institution.

Conflict of Interests

The authors declare no conflicts of interest.

Data Availability Statement

The data that support the findings of this study are available in the supplementary material of this article.

Keywords: 4-nitroimidazole analogs • Antiproliferative activity • Cycloaddition reaction • Hydroximidoyl chlorides • Isoxazoles • Molecular docking study

- [1] S. Poyraz, M. Yıldırım, M. Ersatir, *J. Med. Res.* **2024**, *33*, 839–868.
- [2] S. S. Alghamdi, R. S. Suliman, K. Almutairi, K. Kahtani, D. Aljatli, *Drug Des. Devel. Ther.* **2021**, *33*, 3289–3312.
- [3] P. Sharma, C. LaRosa, J. Antwi, R. Govindarajan, K. A. Werbovetz, *Molecules* **2021**, *26*, 4213.
- [4] G. Ş. Andrei, B. F. Andrei, P. R. Roxana, *Review. Mini Rev. Med. Chem.* **2021**, *21*, 1380–1392.
- [5] C. Deng, H. Yan, J. Wang, B.-s. Liu, K. Liu, Y.-m. Shi, *Arab. J. Chem.* **2022**, *15*, 104242.
- [6] A. J. Karjalainen, K. O. A. Kurkela, *US Patent 45* **1985**, 446, 64A.
- [7] S. Sadeghian, F. Bekhradi, F. Mansouri, R. Razmi, S. G. Mansouri, A. Alireza Poustforoosh, S. Khabnadideh, K. Zomorodian, Z. Zarehshahrabadi, Z. Rezaei, *J. Mol. Struct.* **2023**, *1302*, 137447.
- [8] A. A. Marzouk, A. K. A. Bass, M. S.h. Ahmed, A. A. Abdelhamid, Y. A. M. Elshaier, A. M. M. Salman, O. M. Aly, *Bioorg. Chem.* **2020**, *101*, 104020.
- [9] A. Siwach, P. K. Verma, *BMC Chem.* **2021**, *15*, 12.
- [10] Y.-L. Fan, X.-H. Jin, Z.-P. Huang, H.-F. Yu, Z.-G. Zeng, T. Gao, L.-S. Feng, *Eur. J. Med. Chem.* **2018**, *150*, 347–365.
- [11] D. Davidov, *J. MAB.* **2016**, *22*, 1036–1938.
- [12] E. S. Newlands, M. F. G. Stevens, S. R. Wedge, R. T. Wheelhouse, C. Brock, *Cancer Treat. Rev.* **1997**, *23*, 35–61.
- [13] P. R. Sawyer, R. N. Brogden, R. M. Pinder, T. M. Speight, Avery, *Drugs* **1975**, *6*, 424–447.
- [14] P. D. Crowley, H. C. Gallagher, *J. Appl. Microbiol.* **2014**, *117*, 611–617.
- [15] A. H. Ceruelos, L. C. Romero-Quezada, J. C. R. Ledezma, L. L. Contreras, *Eur. Rev. Med. Pharmacol. Sci.* **2019**, *23*, 397–401.
- [16] R. Meißner, L. Feketeová, E. Illenberger, S. Denifl, *Int. J. Mol. Sci.* **2019**, *20*, 3496.
- [17] J. Fischer, C. R. Ganellin, *Analogue-Based Drug Discovery*, John Wiley & Sons, Hoboken, NJ **2006**, p. 606.
- [18] P. Nyirjesy, J. R. Schwebke, *Future Microbiol.* **2018**, *13*, 507–524.
- [19] J. Thulkar, A. Kriplani, N. A. Agarwal, *Indian J. Pharmacol.* **2012**, *44*, 243.
- [20] M. M. Vichi-Ramírez, E. López-López, C. Soriano-Correa, C. Barrientos-Salcedo, *Future Pharmacol.* **2024**, *4*, 222–255.
- [21] Y. Hu, Y. Shen, X. Wu, X. Tu, G. X. Wang, *Eur. J. Med. Chem.* **2018**, *143*, 958–969.
- [22] N. A. Al-Masoudi, Y. A. Al-Soud, E. De Clercq, C. Paneccoque, *Heteroat. Chem.* **2007**, *18*, 333–340.
- [23] N. A. Al-Masoudi, Y. A. Al-Soud, A. Kalogerakis, C. Pannecouque, E. De Clercq, *Chem. Biodivers* **2006**, *3*, 515–526.
- [24] J. Wang, D.-B. Wang, L.-L. Sui, T. Luan, *Arab. J. Chem.* **2024**, *17*, 105794.
- [25] Y. Shinde, B. Khairnar, S. Bangale, *ChemistrySelect* **2024**, *9*, e202401423.
- [26] A. Sysak, B. Obmińska-Mrukowicz, *Eur. J. Med. Chem.* **2017**, *137*, 292–309.
- [27] G. C. Arya, K. Kaur, V. Jaitak, *Eur. J. Med. Chem.* **2021**, *221*, 113511.
- [28] N. Agrawal, P. Mishra, *Med. Chem. Res.* **2018**, *27*, 1309–1344.
- [29] M. Zimecki, U. Bąchor, M. Mączyński, *Molecules* **2018**, *23*, 272423102724.
- [30] A. M. Eid, M. Hawash, J. Amer, A. Jarrar, S. Qadri, I. Alnimer, A. Sharaf, R. Zalmoot, O. Hammoudie, S. Hameedi, A. Mousa, *BioMed. Res. Intern.* **2021**, *2021*, 6633297.
- [31] S. S. Wazalwar, A. R. Banpurkar, F. Perdihi, *J. Biomol. Struct. Dyn.* **2023**, *41*, 9476–9491.
- [32] N. J. Salgia, Z. B. Zengin, S. K. Pal, *Ther. Adv. Med. Oncology.* **2020**, *12*, 1–9.
- [33] S. Greene, K. Watanabe, J. Braatz-Trulson, L. Lou, *Biochem. Pharmacol.* **1995**, *50*, 861–867.
- [34] R. S. Vardanyan, V. J. Hruby, *Synth. Essen. Drugs* **2006**, 425–498.
- [35] X. Wang, Q. Hu, H. Tang, X. Pan, *Pharmaceuticals (Basel)* **2023**, *16*, 228.
- [36] Y. A. Al-Soud, K. A. S. Alhelal, B. A. Saeed, L. Abu-Qatouseh, H. H. Al-Suod, A. A. H. Al-Ahmad, N. A. Al-Masoudi, R. A. Al-Qawasmeh, *Arkivoc* **2021**, *Viii*, 296–309.
- [37] Y. A. Al-Soud, S. O. W. Saber, A. Shtaiwi, S. O. Alsawakhneh, K. A. Alhelal, Q. F. Salman, L. Abu-Qatouseh, M. A. Khanfar, R. A. Al-Qawasmeh, *Z. Naturforsch. C.* **2022**, *78*, 93–103.
- [38] R. A. Al-Qawasmeh, S. O. W. Saber, Y. A. Al-Soud, M. A. Khanfar, *Z. Kristallogr.- New Crys. Struct.* **2022**, *237*, 207–209.
- [39] S. O. W. Saber, R. A. Al-Qawasmeh, L. Abu-Qatouseh, A. Shtaiwi, M. A. Khanfar, Y. A. Al-Soud, *Heliyn* **2023**, *9*, e19327.
- [40] D. C. B. Da Silva-Alves, J. V. Dos Anjos, N. N. M. Cavalcante, G. K. N. Santos, D. M. D. o. A. F. Navarro, R. M. Srivastava, *Bioorg. Med. Chem.* **2013**, *21*, 940–947.
- [41] K. C. Liu, B. R. Shelton, R. K. Howe, *J. Org. Chem.* **1980**, *45*, 3916–3918.
- [42] W. Willker, D. Leibfritz, R. Kerssebaum, W. Bermel, *Magn. Reson. Chem.* **1993**, *31*, 287–292.
- [43] T. Mosmann, *J. Immunol. Methods* **1993**, *65*, 55–63.
- [44] G. M. Morris, R. Huey, W. Lindstrom, M. F. Sanner, R. K. Belew, D. S. Goodsell, A. J. Olson, *J. Comput. Chem.* **2009**, *16*, 2785–2791.
- [45] M. D. Hanwell, D. E. Curtis, D. C. Lonie, T. Vandermeersch, E. Zurek, G. R. Hutchison, *J. Cheminform.* **2012**, *4*, 17.

Manuscript received: February 16, 2025